SQUID Activities in Europe, Part I: Devices

Alex I. Braginski[1] and Gordon B. Donaldson[2]

(1) Forschungszentrum Jülich, GmbH (FZJ), D-52425 Jülich, Germany

(2) Dept. of Physics, University of Strathclyde, Glasgow G4 0NG, Scotland, UK

E-mail: a.braginski@fz-juelich.de; g.b.donaldson@strath.ac.uk

Abstract – **We present an overview of SQUID research and development in Europe. The tutorial information and historical background are kept at a minimum; we also mention only briefly the theoretical contributions and more fundamental experiments. Rather, we concentrate on practical SQUIDs and SQUID readout and highlight selected recent advances. Today, SQUID itself is a rather mature device. Current research and development work concentrates mostly on satisfying needs imposed by novel applications, which often require more complicated SQUID circuits, including SQUID serial arrays and auxiliary devices on one chip. In closing, we mention the European foundry and current industrial capabilities. Applications are covered by Part II of this overview to be published separately.**

I.   INTRODUCTION

The Superconducting Quantum Interference Device (SQUID) is the subject of a vast literature accumulated since the beginnings over forty years ago. For a detailed presentation of device principles and fundamentals we refer the reader to a recent textbook, which also provides a representative selection of that literature [1]. Here, it suffices to say that SQUID combines the physical phenomena of flux quantization and Josephson tunneling. The device consists of a superconducting loop incorporating at least one Josephson junction (the rf SQUID), typically two (the most popular dc SQUID) and in special cases more (*e.g.*, in quantum bit use). Figure 1(a) shows the symbol of the dc SQUID loop with two Josephson junctions (JJ) conforming to the resistively and capacitively shunted junction (RCSJ) model, and symbolized by crosses. The equivalent circuit of the device, shown in Figure 1 (b), identifies the main SQUID parameters, the loop inductance L_s, the critical current of each of two nominally identical junctions connected in parallel, I_c, the junction shunt resistance R_n, and the external dc current, I_b, biasing both junctions into the voltage state. The shunt assures their nonhysteretic current-voltage (*IV*) characteristic[*]. The critical currents of the two junctions, and thus their *IV* characteristics, shown in Figure 1(c) are modulated by the external flux, Φ_{ex}, which threads the loop. At the current bias I_b and with *changing* Φ_{ex}, the voltage

---

[*] SQUID with hysteretic junctions was also proposed and analyzed, as mentioned in Section IV.

across the SQUID oscillates with an amplitude ΔV and is periodic in the flux quantum $\Phi_0 = 2.07 \times 10^{-15}$ Wb, with a flux-to-voltage transfer function $V_\Phi = \partial V / \partial \Phi$, as shown in Fig. 1(d). Periodic extremes of the voltage modulation occur whenever Φ_{ex} is equal to any integer and half-integer value of the flux quantum. Consequently, the SQUID can be viewed as a transducer for counting flux quanta and measuring the flux *change*. With suitable external flux-locked loop (FLL) feedback electronics, minute flux changes, orders of magnitude below one flux quantum, can be resolved and the quanta counted thus assuring a wide dynamic range for the device.
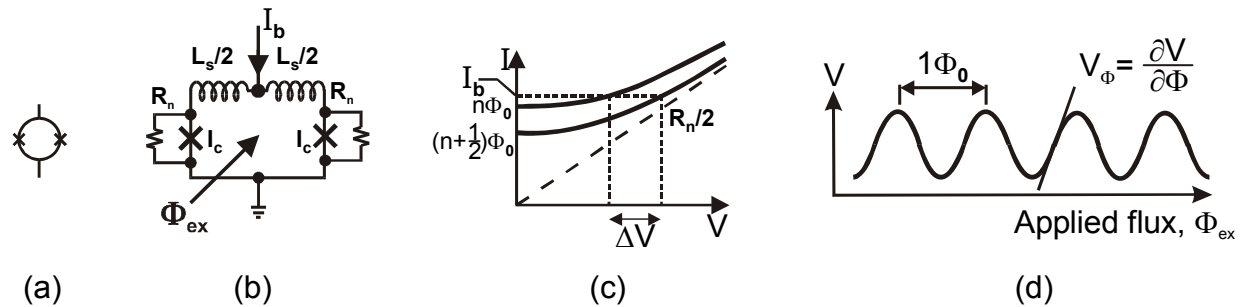

Fig. 1. The dc SQUID: (a) the symbol; (b) the equivalent circuit; (c) the current-voltage characteristics at two extreme flux values; (d) output voltage vs applied flux (signal).

The output voltage of the rf SQUID is similarly periodic in Φ_0. The physical principle of the operation of this device is somewhat different and not discussed here; a detailed discussion of rf SQUID fundamentals can be found in [1].

In the past, SQUIDs served mainly as extremely sensitive magnetic flux and field analog measuring devices, *i.e.*, magnetometers and gradiometers, and were also used as extremely sensitive voltmeters and ammeters. To attain a large effective area threaded by flux and thus high sensitivity to the magnetic field, B, an input circuit consisting of a superconducting flux transformer inductively coupled to the SQUID is usually used. The large area A is provided by a signal pickup coil of inductance L_p. In this case, the SQUID and the multi-turn coupling (input) coil are inside a superconducting shield which screens out undesired signals. The simplified schematic of this circuit, without parasitic inductances and capacitances, is shown in Figure 2.
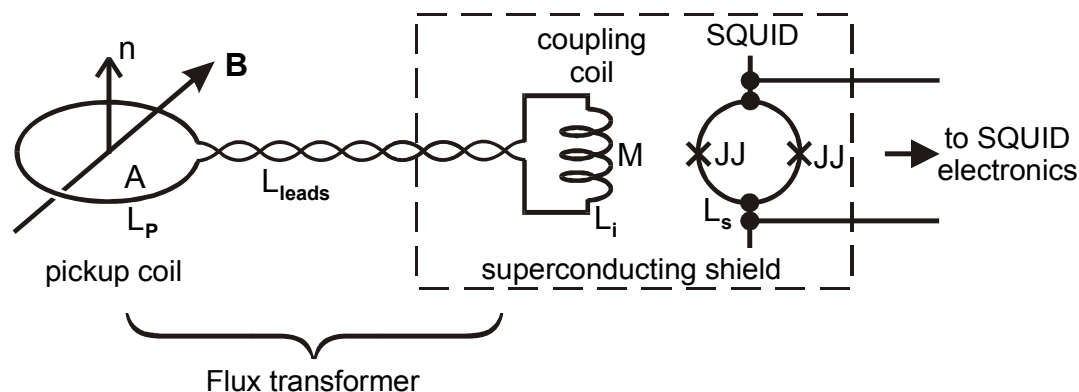

Fig. 2. Schematic diagram of flux transformer inductively coupled to a dc SQUID within a superconducting shield.

Usually, magnetic field from a local source has to be measured in the presence of other field(s) originating from more distant source(s). In such cases a gradiometric pickup coil arrangement makes it possible to suppress the field of these sources. This is illustrated here by the first-order gradiometer shown schematically in Figure 3. Such a gradiometer is obtained when two truly identical pickup coils, separated by distance (baseline) b and having the same normal vector $\boldsymbol{n}$ (thus "balanced"), are connected in series opposite, Figure 3 shows schematically such a first-order gradiometer with $\boldsymbol{n}$ parallel to z axis. In the divergent magnetic field B, the flux values threading the two coils are different: $\Phi_1 > \Phi_2$. Therefore, current $i_T \propto (\Phi_1 - \Phi_2) \propto \partial B_z / \partial z$ will be induced in the flux transformer. A sufficiently distant source produces a uniform field or "common mode". Therefore, $\Phi_1 = \Phi_2$ and $i_T = 0$. When connecting more coils in series opposite with appropriate number of turns, higher order gradiometers can be obtained. Planar coil layouts can fabricated in multilayer thin-film technology.
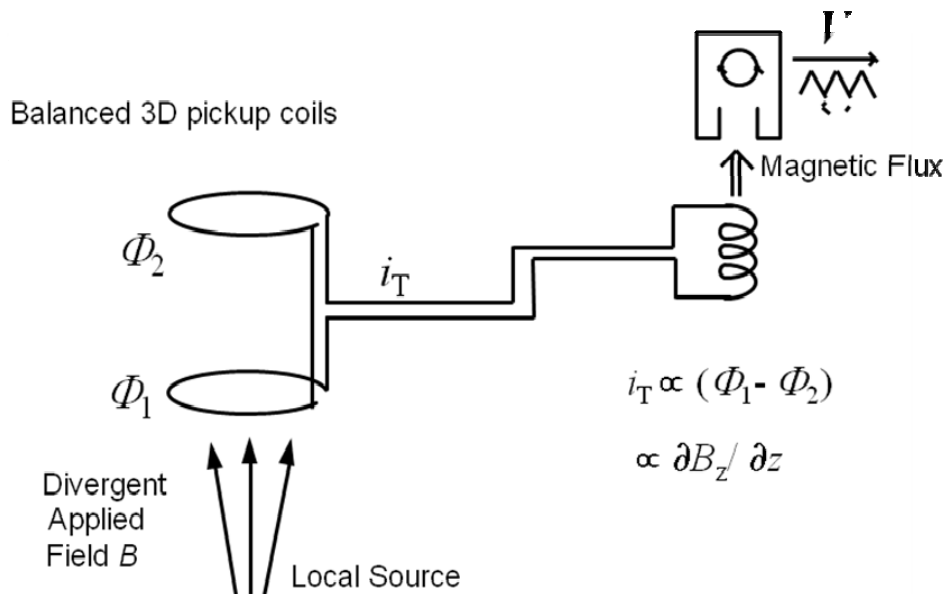

Fig. 3. Schematics of first-order gradiometer. Magnetic flux of the coupling coil threads the SQUID loop placed in a superconducting shield enclosure.

Currently, in addition to traditional magnetometric applications, SQUIDs are of interest as basic cells of analog signal amplifiers and multiplexers, digital RSFQ (Rapid Single Flux Quantum) logic, and lately of qubit (quantum bit) circuits for quantum computing research.

Low-T_c SQUIDs and associated magnetometry are already a mature area, where only slow incremental progress occurs, except for novel applications. High-T_c SQUIDs are still hampered by inadequate and overly expensive technology of high-T_c Josephson junctions, contacts, and multilayer circuits, so that interest in these has subsided after a decade of hectic activities.

Starting with a little of history, we intend here to overview the recent SQUID activities in Europe and highlight potential for future developments. We limit this paper to the area of analog devices and circuits. RSFQ and the qubit research devices are not included. We

mention contributions to theory and basic experiment only briefly, but concentrate on practical SQUIDs, and essentially analog applications. Such applications will be covered by Part II of this overview, to be published in a future issue of ESNF. Our selection is highly subjective and we apologize to all those whose work is neither mentioned nor referenced.

II. HISTORICAL OVERVIEW

The origins of the SQUID and the seminal early work go back to United States in the 1960s where and when the acronym was coined [2,3,4]. Also most of subsequent important research on SQUID performance, design and fabrication technology was done and published there. The first important European contributions we are aware of were those of John Clarke at Cambridge, before he transferred to University of California (UC) at Berkeley: the SLUG (Superconducting Low-inductance Undulatory Galvanometer, leading to the first SQUID picovoltmeter shown in Figure 4, the concept of the flux transformer to dramatically enhance magnetic field sensitivity, and the use of a second SQUID to read out a first-stage SQUID [5,6,7]. With John moving to Berkeley in 1969, his group became a cradle, where, ever since, young European scientists interested in SQUID-related subjects have been finding coaching and inspiration for their future work. In the early years, another such cradle was the University of California at La Jolla, and the first SQUID company spun-off from there, the S.H.E., later known as "Biomagnetic Technologies, Inc.", and eventually as 4-D Neuro-imaging.
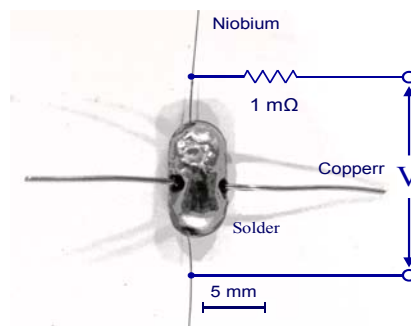

Fig. 4. First SQUID picovoltmeter based on SLUG; device noise 10 fVHz$^{-1/2}$
(courtesy of John Clarke).

In the 1970s and 1980s, several European centers of excellence in SQUID work developed. One of these was Moscow University and the group around K.K. Likharev. Their comprehensive SQUID analysis is incorporated in a book published in Russian and not available in the West [8], but the more important results are presented in [9]. The group contributed also to experimental concepts, for example, proposing and demonstrating the first rf SQUID with a dielectric resonator serving as a tank circuit [10].

In the same period of time, a group around O.V. Lounasmaa (OVL) at Helsinki University of Technology (HUT, Finland), fertilized by OVL's participation in the founding and early phase of S.H.E. activity, initiated work on SQUIDs for biomagnetic applications, which resulted in the creation of a number of worldwide leading centers of activity in dc SQUIDs and such applications, including an industrial spin-off, Neuromag [11]. Developments of

importance for practical dc SQUIDs were also contributed, under the leadership of H. Seppä, by the Technical Research Center of Finland (now VTT). Multiple contributions to the detailed analysis of dc SQUIDs with input structures (coupled SQUIDs) and parasitic elements were made, some of them cited in Section IV. Also many electronics concepts, such as the novel amplifier noise cancellation technique with adaptive, positive feedback originated at VTT [12,13]. This will be mentioned in Section V.

Another center of excellence in SQUIDs and applications (biomagnetic, metrological and others) evolved in Germany in the 1970's, initially through efforts of H.-D. Hahlbom and S.-N. Erné at Physikalisch-Technische Bundesanstalt in Berlin (PTB-Berlin, Germany). Since the late 1980s, significant contributions to planar low-T_c SQUID design and dc SQUID electronics have been made there by Drung *et al*. We mention, for example, the low-noise magnetometers for biomagnetic use and the first concent of direct-coupled, integrated SQUID electronics for SQUIDs with additional positive feedback (APD) [14,15], also mentioned in Section V. In the same period, novel biomagnetic applications were pioneered at PTB under the leadership of H. Koch and L. Trahms. References to SQUIDs in these and other applications are given in Part II of this overview.

Significant SQUID R&D activity was also conducted in several other German institutions, of which we mention the University of Giessen (Ch. Heiden and M. Mück) in conjunction (in the 1990s only) with the Research Center Jülich (FZJ). There, Michael Mück originated the first planar microwave rf SQUID [16]. A continuing center of excellence in low- and high-T_c SQUIDs and applications, with roots going back to times well before the unification of Germany, are the University of Jena (P. Seidel, H. Nowak), and the IPHT-Jena (H.E. Hoenig and H.-G. Meyer, see below). IPHT should be credited with the successful introduction of SQUID detectors to commercial geomagnetic prospecting.

In Italy, early SQUID research and development concentrated mostly in Rome at the University "la Sapienza" (M. Cerdonio *et al*.) and at the CNR Solid State Institute (the Italian National Research Center; I. Modena, P. Carelli, G.-L. Romani *et al*.). Biomagnetism has been one of the major motivations. Macroscopic quantum coherence (MQC) and gravitational wave detector work (GWD) involving SQUID has been also conducted there. The GWD activities continue until present, also at the University of Trento (S. Vitale *et al*.). In the 1980s, Romani transferred from CNR to the University of Chieti, where biomagnetic applications have been pursued ever since. In the 1990s, low-T_c devices for biomagnetism have been developed at CNR-ICIB (Cybernetics Institute) in Naples [17]. Indeed, practical dc SQUIDs developed and fabricated at CNR have been used in all large commercial biomagnetic SQUID systems constructed in Italy. Other activities at Naples CNR have been involving MQC, SQUIDs for magnetic miscroscopy [18], and most recently also nano-SQUIDs. Starting in 1995, high-T_c devices for nondestructive evaluation of materials and structures (NDE) have been pursued at the University of Naples under the leadership of A. Barone.

A significant SQUID research activity developed in the Netherlands at the University of Twente under the leadership of H. Rogalla, J. Flokstra and G. Gerritsma. For many years biomagnetic applications and GWD have been pursued there. The perhaps most significant contribution was the successful development of the DROS (double relaxation oscillation SQUID) intended for GWD readout, which is briefly discussed in Section IV.B.

Among the early pioneers of NDE using SQUID was G.B. Donaldson, (GBD) and his group at Strathclyde University (Glasgow, UK) [19]. This group was also active in biomagnetic applications. The Strathclyde activities have been curtailed with the retirement of GBD, but continue in collaborations with other Scottish groups and with CSIRO, Australia.

In industry, the worldwide first large multichannel SQUID for biomagnetism (37 channels) was constructed and manufactured at Siemens AG under the leadership of H.E.

Hoenig [20]. Figure 5 shows the "Krenikon" system being used to measure functional magnetic fields of human subject's heart and brain. After the "Krenikon" and SQUID-related R&D at Siemens were discontinued in the early 1990s, Hoenig transferred to the newly created "Institut für Hoch-physikalische Technologie" (IPHT-Jena) and was instrumental in establishing there a flourishing SQUID activity, including the European Foundry and an industrial spin-off, "Supracon" [21].

Fig. 5. The "Krenikon" 37-channel biomagnetometer used to measure human subject's heart and brain magnetic field activity (courtesy of H.E. Hoenig and Siemens AG – Sector Healthcare, "MedArchiv").

In 1987, feverish activities following the discovery of the high-T_c cuprates promptly encompassed the SQUID area and resulted in a wave of European contributions, of which only few withstood well the dent of time. One of the first polycrystalline SQUIDs reported was that of Colin Pegrum *et al.* [22]. In the 1990s, one of the more prominent activities in high-T_c SQUIDs, especially in applications, became that at the Research Center Jülich (FZJ), Germany, initially led by late Ch. Heiden, who years ago was also inspired at Berkeley. There, Y. Zhang *et al.* gradually developed what became the now standard design of a sensitive (near microwave) high-T_c rf SQUID [23]. The most robust and sensitive high-T_c dc SQUIDs with Pr-barrier step junctions were developed by U. Poppe and M. Faley of a different Jülich group [24]; these are used in currently custom-manufactured commercial 77 K SQUID systems [25].

III. THEORY AND BASIC EXPERIMENT

The theory of SQUID signal and noise, in the limit of small thermal fluctuations, evolved almost exclusively in the US, except for that of rf SQUIDs, to which J. Kurkijärvi [26], and Likharev *et al.* [9, 27] made significant contributions. Much of rather important work by European authors was actually performed while on postdoctoral or sabbatical stay at

Berkeley. As an example, we cite here Hilbert and Clarke's first systematic work on SQUID rf amplifiers [28]. Recently, Mück, while at Berkeley, demonstrated the extension of amplifier performance to microwave frequencies by inventing the SQUID with microstrip input circuit [29, 30]. Nearly quantum-limited noise was attained at 0.5 GHz, with noise temperatures as low as 50 mK at temperatures below 80 mK [31].

The first conceptually new European SQUID circuit, or rather a readout method, was the relaxation oscillation dc SQUID (ROS), first demonstrated by P. Guttmann [32]. It exploited earlier work by Vernon and Pedersen on relaxation oscillations in hysteretic Josephson junction [33]. More on ROS can be found in Section V. Guttmann's ROS achieved the then record low value of SQUID energy resolution of 3.9×10^{-31} J/Hz. However, shortly thereafter this record was beaten by Cromar and Carelli, who, guided by the noise theory of Tesche and Clarke [34], experimentally investigated low-noise thin-film dc SQUIDs and, for a very low inductance SQUID design ($L \sim 1$ pH) attained energy resolution approaching the quantum limit: 6×10^{-34} J/Hz = 0.9 h [35]. For a coupled SQUID of a hybrid design and somewhat larger inductance of ~ 6 pH (see Section IV) they attained 71 h. This work was one of a number of milestones establishing the dominance of the dc SQUID, rather than the rf SQUID, as the most sensitive flux detector.

In 1990s, to further the understanding of dc and rf high-T_c SQUIDs, B. Chesca developed analytical solutions based on the Fokker-Planck equation, and useful also in the limit of large thermal fluctuations [36,37]. For the rf SQUID, some surprising predictions of that theory were validated experimentally by Zheng et $al.$ [38]. For dc SQUID, extensive numerical simulations of coupled Langevin equations, also in the limit of large thermal fluctuations, were performed in a work initiated at Berkeley by R. Kleiner [39,40]. In contrast to analytical theory, valid in limited range of SQUID parameters, the simulation results are applicable in a broader parameter range. Most recently, Kleiner et $al.$ published also the first ever extensive simulations of the rf SQUID [41, 42]. The effect of dc SQUID asymmetry was studied by Koelle et $al.$ both numerically and experimentally [39], and also by Testa et $al.$, who showed that for certain dc SQUID parameters asymmetry can lead to noise reduction [43].

In 1997, Carelli et $al.$ proposed a novel $absolute$ magnetometer consisting of a series array of dc SQUIDs with incommensurable loop areas [44]. Simulations and preliminary experiments confirmed the feasibility of such a device with non-periodic voltage $versus$ flux characteristic. Unfortunately, the results were less than impressive due to low number(s) of SQUIDs in the arrays, not exceeding 7. Even earlier, a study of large Josephson junction arrays with long-range interaction resulted in experimental data quite suggestive of such characteristics [45]; Carelli et $al.$ were probably unaware of that work. In 1999-2001, Oppenländer et $al.$ performed a systematic theoretical analysis of 1D junction arrays connected to form a one-dimensional parallel or series array such that there are, respectively, ($N - 1$) or $2N$ individual superconducting loops of arbitrary shapes; N is here the number of junctions [46, 47]. This analysis, including numerical modeling of array's nonlinear dynamics, resulted in what the authors named superconducting quantum interference filter (SQIF). In the parallel array resistive mode ($I > I_0$), all the junctions oscillate with the same Josephson frequency, f_B, which in general can be a function not periodic in Φ_0. The authors showed that with junctions conforming to the RCSJ model, f_B is solely a function of the array geometry. For certain loop size distributions, analogous to unconventional grating structures, Josephson oscillations result in time averaged voltage response exhibiting a singularity, $i.e.$, a sharp global minimum at $\boldsymbol{B} = 0$, which corresponds to maximum coherence of the array. This should be so in both parallel and series arrays. Subsequently, the Carelli's concept of an $absolute$ magnetometer, was convincingly demonstrated experimentally in both parallel and series array configuration [48,49]. These demonstrations confirmed very well the theoretical

predictions. Figure 6 compares the simulated voltage response of a SQUID ($N = 2$) with that of a periodic 1D parallel array ($N = 11$) and of a 1D array with an unconventional grating structure ($N = 18$), where the voltage is a unique function of applied flux. In subsequent years, multiple modeling and experimental contributions by original authors followed, also in collaboration with two other European groups. These will be reviewed in Section IV.
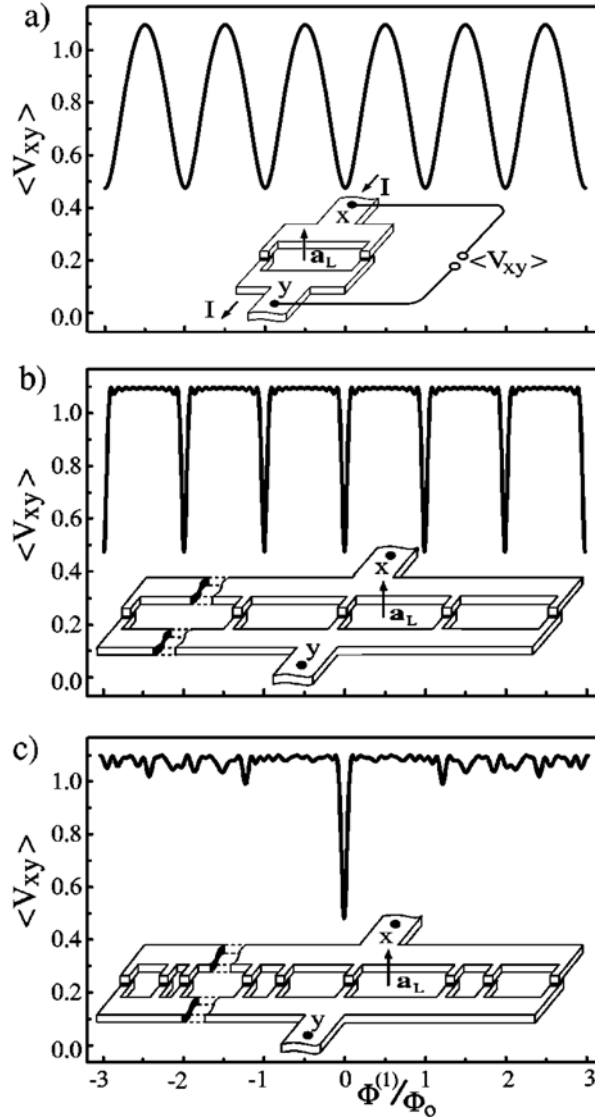

Fig. 6. Voltage response V_{xy} in units of I_cR versus external flux through largest area element of interferometer a_L with N overdamped junctions for bias current $I = 1.1\ NI_c$ and vanishing inductive coupling; (a) symmetrical SQUID ($N = 2$), (b) periodic 1D array (N = 11), (c) 1D array with unconventional grating structure. The loop areas in (c) are randomly distributed between 0.1 and $1.0a_L$, but with the same total area as in (b) [46] (© APS, with permission).

A valuable experimental contribution to understanding the $1/f$ noise behavior of high-T_c SQUID, and flux trapping in them, was the visualization of vortices in SQUID washers, and other thin-film SQUID elements by low-temperature scanning electron microscopy (LTSEM) [50]. The underlying calculations of vortex coupling to round washer SQUID were first done analytically by Humphreys [51] and for a square washer via numerical simulations by

Khapaev *et al*. [52]. By correlating flux noise data with the observed spatial distribution of vortices an average vortex hopping length was estimated at ~ 10 nm.

IV. PRACTICAL SQUID TECHNOLOGY AND DESIGN

A. Technology and Magnetometers

The Nb/Al$_2$O$_3$/Nb junction fabrication technology pioneered by Rowell, Gurvitch and Geerk at Bell Laboratories [53], and the coupled thin-film washer SQUID with integrated planar input coil developed at IBM by Jaycox and Ketchen [54] became the technological foundations of modern low-T_c dc SQUID magnetometers. This multilayer thin-film technology enabled modern designs of numerous practical dc SQUIDs, many of which were developed or co-developed in Europe. As examples we mention here two variants of a planar multiloop dc SQUID inspired by the original Zimmerman concept [55]. The first was the mentioned above hybrid approach of Cromar and Carelli [35], later improved by Carelli *et al*. [56]. The authors placed a planar multiloop SQUID inside of a multi-turn input coil of a flux transformer. The other, simpler and more practical, originated at PTB-Berlin and became a design used in their sensitive biomagnetometers [15, 57]. This so-called "cartwheel" or "Drung's wheel"is shown in Figure 7, in both a low-T_c and high-T_c version.
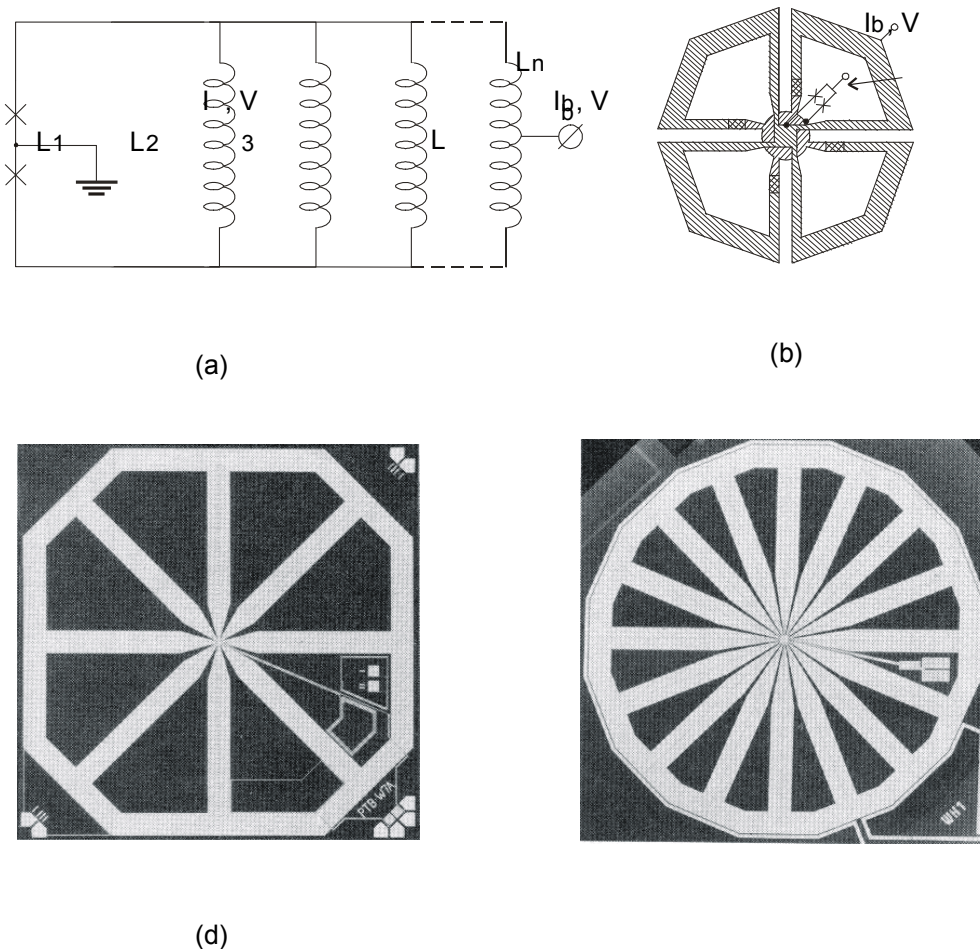

(a)

(b)

(d)

Fig. 7. The planar multiloop magnetometer: (a) simplified schematics, (b) simplified layout showing the SQUID junctions, (c) microphotograph of the mature low-T_c version [57], (d) an experimental high-T_c version [58], which did not find practical application (© SuST, IOP with permission).

In the current decade, stimulated by the need for robust and easy-to-use SQUID amplifiers, which could also be operated in the temperature range below 1 K and down to 10 mK, PTB developed a whole family of complex devices with several hundreds of SQUIDs in series arrays and auxiliary components on chip. Some of these are available commercially. Just one recent example is the two-stage, on-chip integrated device consisting of an input SQUID with additional positive feedback, and the second stage shunted series array of 16 SQUIDs serving as a low-noise preamplifier. It is briefly described in the Forum paper ST2, to which we refer our readers.

In the search for ever more sensitive devices, Seppä et al. analyzed dc SQUID operation with unshunted, hysteretic junctions [59]. The promise of even lower noise and a high gain appeared high, but (to the best of our knowledge) was not confirmed by practical results.

High-T_c technology, when used for SQUID fabrication, is usually that of junctions created at a bicrystal boundary [60]. However, the most stable in time and largely self-shielded are ramp or edge junctions with Pr barriers pioneered by Gao et al. [61]. In this decade, such junctions have been used in magnetometers, and implemented in some commercial SQUID systems [25]. For very sensitive high-T_c coupled magnetometers a flux transformer must be used. In this case, the flip-chip configuration is a practical solution, due to the relative immaturity of the multilayer fabrication technology and the resulting low yield. Of such devices, the most sensitive to date have been those developed by Faley et al. [24].

For rf SQUIDs, Kornev et al., introduced the already mentioned rf SQUID with a dielectric resonator [10], which later, in a planar high-T_c version developed by Zhang et al. [23] became a relatively mature and simple device.

European authors and groups contributed significantly to the detailed design analysis of low-noise coupled dc SQUIDs, taking into account the effects of parasitic inductances and capacitances. The parasitic elements create the possibility of deleterious LC resonances in the SQUID dynamics. For the bare dc SQUID this was first analyzed by Ryhänen et al. [62]. For integrated thin-film coupled SQUID the input coil deposited on top of the washer introduces a large parasitic capacitance C_p across the SQUID inductance. The resulting resonances were analyzed by Knuutila, Seppä et al. [63, 64, 65], and minimization of C_p by a suitable layout was shown [66]. Methods of damping these resonances by appropriate shunts and damping resistors, but without affecting the noise were demonstrated [67], also for high-T_c SQUID [68]. More details on parasitic effects and the related references can be found in [1].

A problem in practical applications is flux trapping even in well-shielded low-T_c SQUIDs. Therefore, encapsulated commercial sensors as a rule contain a heater for flux expulsion by heating just above T_c. One of the proven remedies reducing flux trapping in low-T_c devices is to design coupled SQUIDs with junctions placed near the outer edge of the junction, outside of the integrated input coil. This was shown, for example, by Penttilä et al. [69]. These authors were also probably first to observe effectiveness of MgB_2 shielding when operating a low-noise low-T_c SQUID with a cryocooler.

B. Gradiometers

While gradiometers measure gradients, their main use is to suppress undesirable signals from unwanted, more distant signal sources, the so-called common mode (see Section I). For quite a long time, three-dimensional axial (radial) coil gradiometers wound of suitable superconducting wire were generally used in practical applications, although planar,

lithographically fabricated gradiometers can offer much better common mode rejection (CMR). The first low-T_c thin-film planar first-order gradiometer was demonstrated, still in the primitive lead (Pb) technology, by G.B. Donaldson (GBD) *et al*. while at Berkeley [70]. A practical low-noise biomagnemoter sensor developed at HUT at the beginning of 1990s was the integrated planar gradiometer pair measuring the orthogonal tangential derivatives $\partial B_z / \partial x$ and $\partial B_z / \partial y$ of the magnetic field B_z [71]. It became the workhorse in whole-head brain biomagnetometers now manufactured by Elekta Neuromag [11]. Details of these gradiometers are presumably proprietary as they haven't been published.

Another successful planar gradiometer design fabricated in the Nb/Al$_2$O$_3$/Nb technology is that of a highly symmetric multiloop SQUID developed by Stolz *et al*. for geomagnetic exploration, where signals induced by motion and rotation in Earth's field should be suppressed [72]. This gradiometer has a relatively large effective pickup area, and consists of four pairs of washers connected in parallel to keep the SQUID inductance below 300 pH[†]. The washers in the pairs are connected in series and form a first-order gradiometer. Figure 8 shows one fourth of the equivalent circuit of this SQUID, while Figure 8 is a microphotograph of the central part of the SQUID chip with four 7-turn input coils partly visible. With further proprietary improvements this gradiometer chip became the workhorse of the highly successful SQUID-based commercial mineral exploration systems described in Part II of this overview.
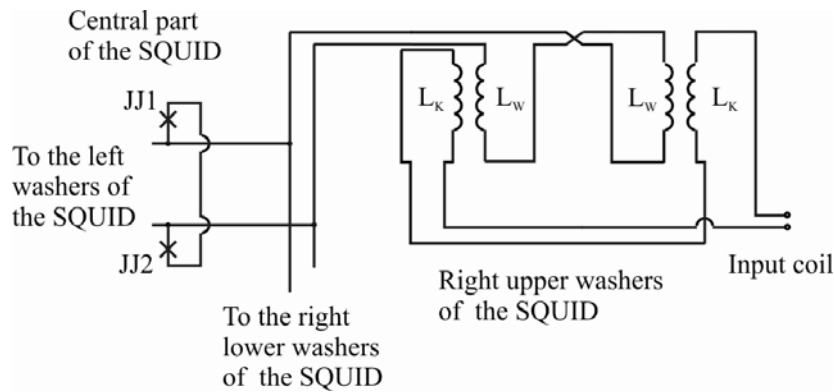

Fig. 8. Part (1/4) of the simplified gradiometric SQUID equivalent circuit, without parasitic inductances shown [72] (© SuST, IOP with permission).
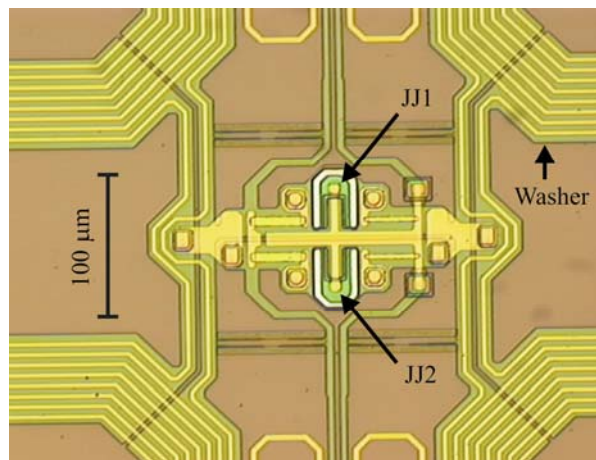

Fig. 9 Microphotograph of the central part of the gradiometric SQUID of Figure 6 [72] (© SuST, IOP with permission).

[†] The inductance of single washer loop is approximately 2,600 pH.

While at present the IPHT systems used in geomagnetic exploration are equipped exclusively with low-T_c gradiometers derived from the design described above, the desire to eliminate the logistic effort required to supply liquid helium to the exploration site is naturally strong. Therefore, Schultze *et al*. developed a highly balanced single-layer high-T_c gradiometer, which has a CMR of nearly 4000, and can be tilted and rotated in Earth's magnetic field [73]. To the best of our knowledge, a commercial exploration system equipped with such gradiometers is in development at IPHT and Supracon.

The first single-layer YBCO high-T_c gradiometers were those developed by Knappe *et al* and Zakosarenko *et al*. [74,75]. One of the main problems of such gradiometers is the magnetometric signal from a small-loop SQUID needed to configure the single-layer device. Figure 10 shows the schematic diagram (a) and the layout (b) of such a gradiometer [76]. The detail (c) represents the layout of the small-loop SQUID, which is the source of the magnetometric (unbalanced) signal. Multilayer gradiometers were experimented with, but the fabrication technology remained immature. Approaches to reducing this signal significantly by using anti-parallel-configured, single-layer SQUID structures were pursued by GBD's group. Eulenburg *et al*. and Carr *et al*. attained gradiometer balances on the order on 10^5, (CMR = 10^5), an order of magnitude improvement over single-SQUID device designs [77,78].
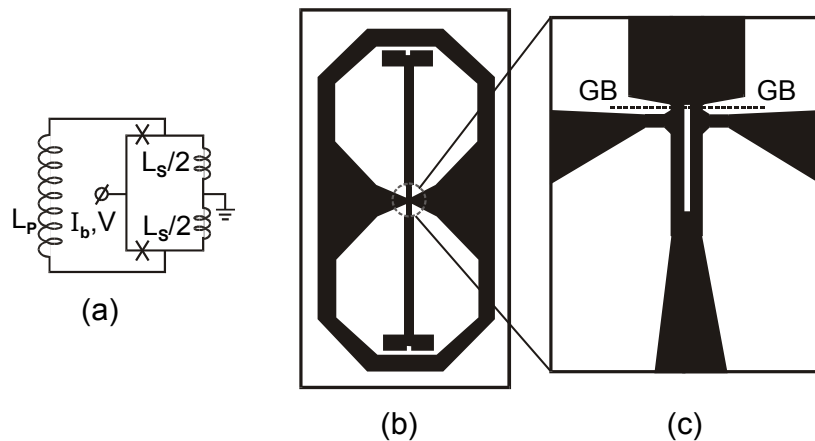

Fig. 10. High-T_c planar dc SQUID galvanometric gradiometer: (a) schematic diagram, (b) layout, (c) detail showing the small-loop grain-boundary (GB) SQUID [76] (© SuST, IOP, with perm.).

C. *Superconducting Quantum Interference Filters*

As is often the case, the demonstration of these entirely new devices, conceived largely through theoretical analysis (see Section III), was met with some skepticism in the SQUID community. So the Tübingen University group around Nils Schopohl, who refined the Carelli *et al*. concept [44], had a comfortable few years to thoroughly investigate SQIF structures, both by modeling and experimentally, without much external competition. Part of their work was done in collaboration with Schultze *et al*. of IPHT-Jena, where first high-T_c SQIFs were demonstrated [79,80], and with Kornev *et al*. of Moscow University, where issues of oscillation linewidth and noise were investigated numerically [81]. These three groups contributed the bulk of all the SQIF work to date. Figure 11 shows the experimental voltage

response to applied field, B_{ext}, of an early parallel SQIF with $N = 30$ [49]. Indeed, the response shows a voltage dip singularity near $B_{ext} = 0$.
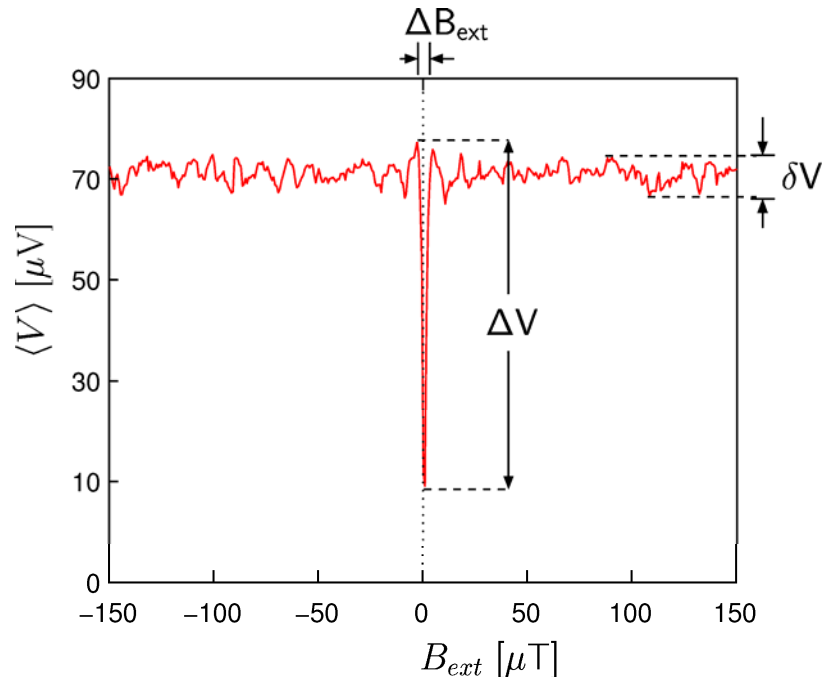

Fig. 11. Typical experimental dc voltage response to external field of an early parallel SQIF with $N = 30$ (Courtesy N. Schopohl). Three important SQIF parameters are indicated (see text).

Already in the early work, the basic rules for a functional and well-performing SQIF were formulated [44, 46]. Most essential is the proper selection of the loop size distribution. These loops have to be incommensurable, the ratio of largest to smallest loop area must be very high, and the distribution such that no distinct size is preferred.

The theoretical expression for a bare (uncoupled) parallel SQIF voltage noise indicates that it should scale with the square root of the number of junctions, $\sqrt{N}$, as should be expected [49]. As the transfer function $\partial V/\partial B$ should scale with N, high N values are beneficial for high signal-to-noise ratio, SNR. In magnetometer application, an appropriate flux focusing structure or flux transformer is required to attain field sensitivity competitive with that of SQUID magnetometers.

Generally, other than low noise and high SNR, a practical SQIF magnetometer should exhibit a possibly high output voltage swing ΔV, high linearity, high transfer function $V_B = \partial V/\partial B \cong \Delta V/\Delta B_{ext}$ and minimal signal variance δV outside the singularity in the $V(B_{ext})$ dependence (see Figure 11). Recent simulations by Kornev *et al*. have shown that in a differential scheme of two parallel SQIFs with arrays oppositely frustrated by applied magnetic field δB_{ext} a linearity of 100 to 120 dB[‡] should be attainable [82], see ST51 .

For the early experimental low-T_c bare device of Figure 11, the calculated minimum white field noise was ~ 600 fT/Hz$^{1/2}$ while the experimental upper limit was 5 pT/Hz$^{1/2}$. A bare serial SQIF with 174 loops exhibited $\Delta V = 9.4$ mV and $V_B = 18700$ V/T [83]. The first demonstrated practical application in field of a low-T_c SQIF amplifier has been in a submillimeter wavelength camera for astronomy, see ST-113. Details of this device remain proprietary at present.

[‡] Linearity was determined from the harmonics content.

Thus far, more experimental data have been published on high-T_c SQIFs than on low-T_c devices, although the latter should offer a much better performance. One reason is that all SQIFs exhibit high tolerance of fabrication-related parameter spreads. Furthermore, SQIF investigators saw early on the prospect of highly sensitive preamplifiers for application in high-performance MHz and GHz range communication antennae and other mobile applications. For such applications, a high-T_c device can be more competitive, in spite of less impressive performance parameters, and can be operated with cryocoolers even in unshielded environments [84]. Indeed, the development of mobile antennae is pursued in an industrial venture [85]. In experiments with high-T_c SQIFs having 100 to 200 loops, the dynamic range per unit bandwidth was 120 dB/Hz$^{1/2}$ [83].

Schultze *et al.* investigated optimization of high T_c SQIF magnetometers on bicrystal substrates [86]. That work included both direct-coupled pickup loops and suitable single-layer flip-chip flux transformers coupled to all SQIF loops. That required using a serial rather than a parallel device. The best coupled performance at 77 K of a serial SQIF with 95 loops was as follows: voltage swing ΔV = 0.7 mV, transfer function V_B = 84 µV/nT, and white noise (field resolution) B_N = 65 fT/Hz$^{1/2}$ at 1 Hz. While the design value of B_N = 27 fT/Hz$^{1/2}$ at 1 Hz was not attained, the measured field resolution was certainly comparable to that attained by high-T_c dc SQUIDs with bias-reversal electronics. Figure 12 shows the layout of this magnetometer.
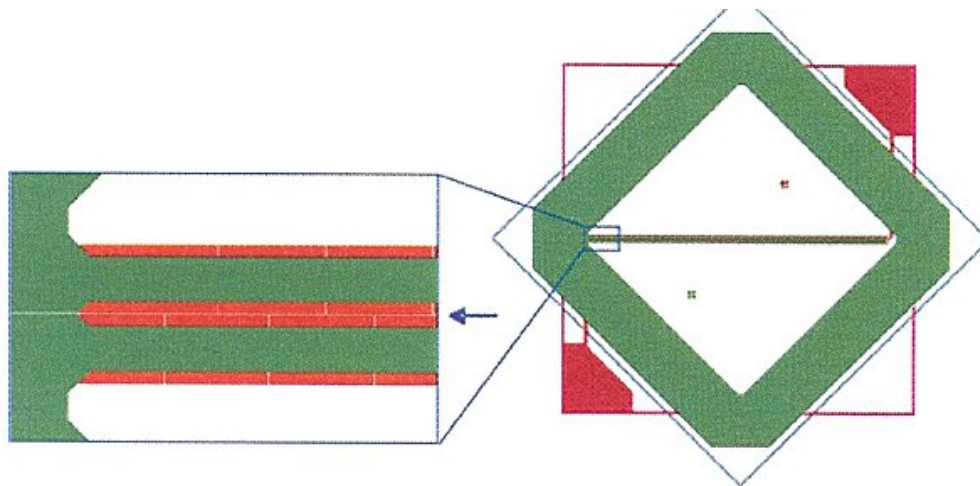

Fig. 12. Layout of the "best" serial SQIF magnetometer with single-layer flip-chip flux trans-former. The SQIF itself is the horizontal dark grey diagonal bar within the square green pickup coil loop. Left: detail of the transition from pickup coil to coupling coil situated above flux-focusing structures of the bare SQIF (5 loops out of 95 are visible). The grain boundary is marked by the blue arrow [86] (© SuST, IOP, with permission).

V. READOUT ELECTRONICS

A. Fundamentals

An external circuit is needed to quantitatively read out the SQUID signal corresponding to the detected magnetic flux change,. This need for external, usually room-temperature, electronics has been perceived since the beginning, and already one of the earliest devices (the SLUG) had a feedback loop to linearize its response to the applied current and detect signal changes corresponding to less than a flux quantum [7]. The flux- or current-locked feedback loop is

the most essential feature of any such electronics, whose principles and detailed analysis are presented in [87,88]. A schematic diagram of an analog circuit with flux locking feedback is shown in Figure 13. In the version shown, the SQUID output is coupled inductively via a transformer to a low-noise (pre)amplifier, while the detection occurs with the help of flux modulation using the oscillator and lock-in detector seen in the schematics. The integrated output is recorded, usually in digitized form, and fed back to the SQUID, which thus functions as a null detector.   In addition, the electronics box contains a dc power supply for biasing and settings control.   Contemporary low-noise SQUID electronics, permits the resolution of minute flux changes, down to the order of $10^{-7} \times \Phi_0$ for the best low-T_c SQUIDs, and large signals, equivalent to many flux quanta can also be measured. The dynamic range of typical analog electronics is in excess of 120 dB. Hybrid electronics, with a 32 bit digital counter of individual quanta might have a dynamic range of approximately 190 dB.
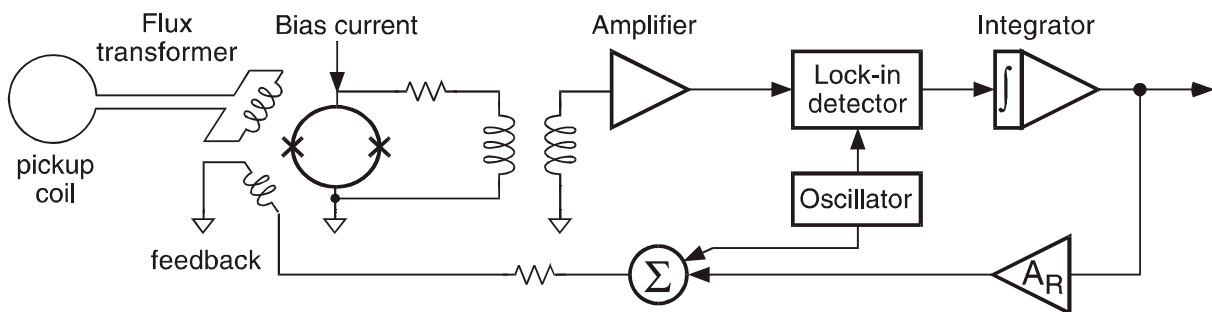

Fig. 13. Schematic diagram of the analog flux-locked loop (FLL) electronics.

B. Direct-coupled Electronics and Additional Positive Feedback

A major European contribution to modern SQUID electronics is the direct-coupled dc SQUID electronics first introduced by Drung *et al*. It eliminates the transformer and flux modulation shown in Fig. 13 to attain a wider bandwidth, while the SQUID sensitivity is enhanced via the additional positive feedback (APF) [14,15], a development, which, with an optional bias reversal reducing the $1/f$ current noise of high-T_c SQUIDs, was also licensed and transferred to industry [89]. The currently attained performance of such electronics, model XXF-1, is presented in [90] and in ST2.

The APF in Drung's electronics reduces the effect of room-temperature amplifier noise through higher $V_\Phi = \partial V / \partial \Phi$ at the SQUID's operating point. An alternative use of APF was introduced by Seppä, who pioneered the adaptive noise cancellation (NC) method [12,13,91]. Here, the SQUID is voltage–biased with amplifier in transimpedance mode, which is also advantageous for linearization of the SQUID response. In this amplifier mode, the amplifier voltage noise is also effectively suppressed. The Seppä-style electronics is the workhorse of large biomagnetic multichannel systems manufactured by Neuromag [71].   A very enlightening comparison of the two ways of using APF was recently published [92]. Figure 14 compares the effect of the two APF uses on simulated voltage-flux characteristics of the SQUID. In the current-biased SQUID response, introduction of APF results in unchanged amplifier voltage noise contribution, but greater voltage gain for a given flux change due to steeper positive slope. In the voltage-biased response the slope steepness doesn't change, but the amplifier voltage noise contribution is reduced on the positive slope and enhanced on the negative, while the linearity is improved and the usable flux range greater, as indicated by green arrows.

Several novel concepts implemented in PTB's XXF-1 permitted to attain the record-wide bandwidth of direct-coupled closed-loop FLL (20 MHz), close to the theoretical limit given by transmission line delay within FLL, and without noise degradation. The amplifier bandwidth of about 50 MHz was attained by creating a composite amplifier consisting of a slow dc amplifier in parallel with a fast ac amplifier. Bandwidth is an essential limitation, for example when using the electronics with SQUID-based multiplexers for cryogenic radiation detector arrays.   Indeed, this new application became the main driver for continuing development of SQUID electronics. The XXF-1 operate with two-stage SQUIDs and series SQUID arrays, and are thus potentially suitable for transition-edge-sensor (TES) readout in astronomy applications. With a two-stage SQUID, the energy resolution of 30 h at 4.2 K and 2.3 h at 0.3 K was attained. The additional advantage of these electronics is the very small size: for example, the whole FLL board of XXF-1 is only 130 x 43 mm, so that it can be mounted directly at the warm end of the SQUID probe, thus minimizing the distance between the SQUID(s) and the readout.
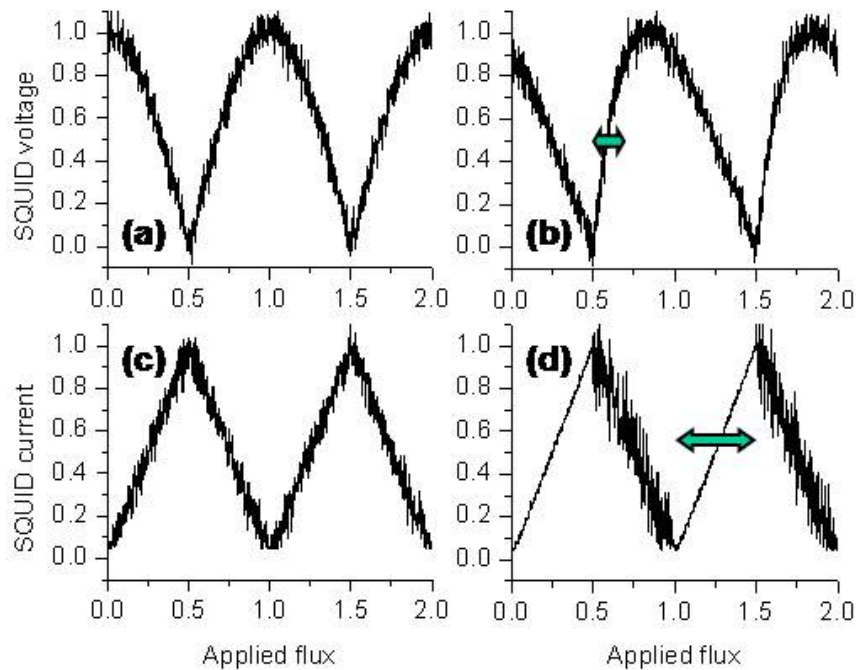

Fig. 14. Simulated response of a SQUID with either current (a, b) and voltage bias (c, d) and exaggerated readout amplifier noise: comparison of effects of APF use; (a, c) without (b, d) with APF [92].
In (b, d) the usable, sufficiently linear flux range is indicated by green arrows. (© SuST, IOP, with permission).

C. Cryogenic Preamplifier and Wide-bandwidth Cryogenic FLL

A possible way to further reduce the noise of room-temperature electronics is to use a cryogenic preamplifier. For some years that was an extreme measure sometimes used for rf and microwave SQUIDs, or dc SQUIDs at radio frequencies, where the noise of the entire system is usually limited by the preamplifier noise [87]. An example of cooled preamplifier using HEMT and MESFET transistors is that introduced by Mück *et al.* in conjunction with a 1.7 GHz microwave SQUID [93]. The whole system open-loop energy resolution at 4.2 K was about 100 h, a record for an rf SQUID. Unfortunately, the main problem with using such cryogenic preamplifiers is their high power consumption, usually prohibitive at 4.2 K and certainly not acceptable at even lower temperatures.

Recently, Kiviranta was first to demonstrate a cryogenic SiGe bipolar transistor preamplifier for use with direct-coupled dc SQUID readout of signals below rf frequencies [94,95]. The main advantage of the SiGe heterojunction bipolar transistors (HTs) is their $1/f$ noise lower than that of HEMTs, but also lower power consumption, with indications it can be even in sub-mW range. The measured open-loop flux noise level with such transistor was, approximately, 0.4 $\mu\Phi_0\mathrm{Hz}^{-1/2}$ at 4.2 K [95].

The main motivation for using a cryogenic preamplifier is presently the need of broad bandwidth and high slew rate (in addition to low noise) of flux-locked electronics for large detector array readouts with multiplexers, especially frequency division multiplexers (FDMs). The cryogenic amplifier can be placed very close to the SQUID, resulting in the reduction of the FLL loop delay, which as a rule is dominated by the transmission line to room-temperature electronics. Lower delay translates into broader bandwidth and higher slew rate.

Both Kiviranta and Drung independently demonstrated this approach at nearly the same time [92,96], but their published results should still be viewed as preliminary. Also both authors independently invented the effective approach to SQUID linearization at high frequencies, which Kiviranta calls current-sampling feedback [92], while Drung prefers the term output current feedback (OCF) [97]. Essentially, the current is used as output rather than voltage. The comparison of the standard direct-coupled FLL principle with that of SQUID linearization by OCF is shown in Figure 6 of ESNF paper RN-9. Drung demonstrated this idea by using a SQUID series array amplifier with up to 640 SQUIDs in a series-parallel configuration, Kiviranta with a cryogenic CMOS switch and a room-temperature amplifier.

According to Drung, in his cryogenic feedback experiments to date, bandwidth and slew rate were comparable with either cooled semiconductor or SQUID array amplifiers [98], representing an order of magnitude improvement over the best XXF-1 results. The static feedback range was significantly higher with semiconductors than with SQUID array OCF, but the power dissipation was also higher, by 5 orders of magnitude.

We note that SQUID arrays also represent a much greater technological challenge than single SQUID. Large SQUID circuits require a refined fabrication technology with narrow linewidths and junction tolerances. While the parameters presented in [97] are already impressive, the cryogenic FLL results still represent work in progress, with no definite performance limits attained up to now. Of course, neither the Kiviranta nor the Drung cryogenic FLL has been implemented in practical applications, as yet.

D. Relaxation Oscillation Dc SQUID

As mentioned in Section III, Guttmann was the first to develop the concept of ROS [32]. It consists of a dc SQUID with hysteretic junctions, which as a whole is shunted by a resistor R_sh and inductor L_sh in series. The SQUID itself behaves like a junction which has stable and unstable branches. Relaxation oscillations occur if the ROS is biased above the critical current, I_c, and its load line with the shunt intersects the unstable subgap voltage branch. In this case, a stable working point in the voltage state is not possible and the voltage across it must oscillate continuously between the junctions' gap voltage and zero. The frequency of oscillations and the duty cycle are a function of the bias current and $I_\mathrm{c}(\Phi_\mathrm{ex})$. Therefore, the ROS can be used as a simple flux-to-frequency (or flux-to-voltage) converter. A simple frequency-modulated readout is thus possible [99].

Improvements to ROS, the balanced ROS [100] and the simplified double ROS (DROS) [101] were subsequently investigated and, especially in the case of DROS, demonstrated very high transfer coefficients $\left|V_\Phi\right| \Rightarrow \partial V_\Phi/\partial\Phi$. Figure 15 shows the schematics of two

alternative DROS implementations, (a) with reference SQUID and (b) with reference junction. Figure 15 (c) shows the step-like V versus $\Phi_{ex} = \Phi_a$ characteristic of DROS, which at the operating point results in high $\lvert V_\Phi \rvert$. However, the relaxation oscillation frequency must be very high, in the microwave range, to attain low noise and high sensitivity [102]. The DROS has been used in experimental GWD systems being developed by Twente researchers.
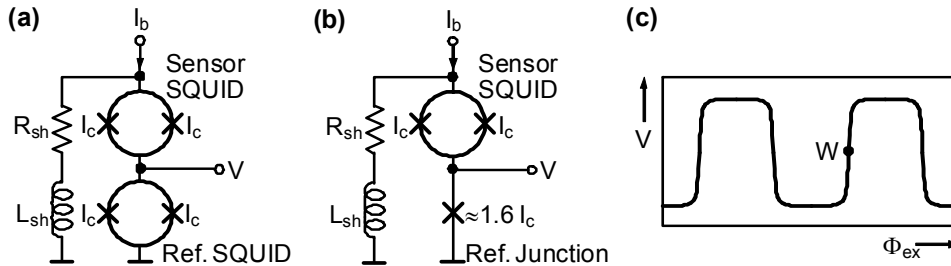

Fig. 15. DROS schematic circuits: (a) with reference SQUID, (b) with reference junctions; (c) the steplike $V - \Phi_{ex}$ transfer function with operating point W. Adapted from [87], Fig. 4.12 (© Wiley-VCH with permission).

In addition to the DROS, digital SQUIDs can be seen as alternative readout schemes. Because of their potential for very high dynamic range and slew rate they have been pursued in many alternative versions, the most sophisticated using the rapid single flux quantum (RSFQ) logic approach involving a decimation filter. However, only rather simple comparator circuits were fully operational. A recent European digital SQUID study was motivated by earthquake monitoring in the presence of high-level magnetic disturbances [103]. The demonstrated SFQ SQUID itself is insensitive, but in combination with an analog SQUID the authors expect to attain both the dynamic range and sensitivity in a hybrid device.

VI. EUROPEAN FOUNDRY AND INDUSTRIAL SQUID FABRICATION

A European foundry fabricating customer-designed SQUID chips exists at IPHT-Jena [104]. It can fabricate both low-T_c and high-T_c SQUID chips of designs conforming to this foundry rules. SUPRACON, a small company spun-off from IPHT-Jena, is marketing SQUID chips adapting its own designs to customer needs [21]. They also manufacture direct-coupled SQUID electronics. Also MAGNICON fabricates SQUID chips and electronics, both on PTB license [89]. The CNR of Naples fabricates SQUID chips for all the Italian biomagnetic systems, and VTT of Espoo, Finland, for all the Finnish biomagnetic systems fabricated by Electa Neuromag. However, neither of these two functions as a regular SQUID foundry. With reference to the ESNF paper RN-9, we note that the trend towards more complicated SQUID circuits on one chip requires that better fabrication equipment, especially for photolithography, be accessible to the foundry and small industrial manufacturers.

VII. CONCLUDING REMARKS

European authors and groups contributed significantly to the development of practical SQUIDs, SQUID electronics, and of applications to be discussed in Part II. However, of all the novel device concepts originated in Europe, it is the SQIF which might turn out to be most important in the future. While SQIF devices are still in a rather early stage of development, we believe there is bright future for their use in diverse applications.

Currently, low-T_c SQUIDs are still the workhorses in most applications, in spite of considerable efforts expended during the past decade to develop practical high-T_c SQUIDs. The main reasons for avoiding these are the still immature high-T_c fabrication technology, especially of multilayer devices, high level of flux trapping in high-T_c thin films, and high cost related to expensive single- and bicrystal substrates and low fabrication yields. Low- and high-T_c SQIFs are much more tolerant to junction and layout parameter spreads, hence their additional advantage. In any event, the current trend towards more complicated SQUID circuits on chip, including SQUID arrays and auxiliary devices, presents new challenges for low-T_c fabrication technology (essentially Nb/AlO$_x$/Nb). Due to the rather antiquated equipment currently available, the resulting linewidth and reproducibility are well below standards of semiconductor manufacturing. However, independent of the necessary fabrication equipment upgrade, the nanometer thick Josephson junction AlO$_x$ barriers will always impose insurmountable limits to narrowing junction critical current tolerances.

While in the past decade biomagnetometer requirements were the main drivers in practical SQUID and electronics progress, SQUID readout of large radiation detector arrays has recently taken over that role.

ACKNOWLEDGEMENTS

REFERENCES

[1] J. Clarke and A.I. Braginski (Eds.) *The SQUID Handbook*, Wiley-VCH, Weinheim, vol. I,II, (2004 and 2006).

[2] R.C. Jaclevic, J. Lambe, A.H. Silver, J.E. Mercereau, "Quantum interference effects in Josephson tunneling", *Phys. Rev. Lett*. **12**, 139 (1964).

[3] A.H. Silver and J. E. Zimmerman, "Quantum states and transitions in weakly-connected superconducting rings", *Phys. Rev*. **157**, 317 (1967).

[4] J. E. Zimmerman and A.H. Silver, "Macroscopic quantum interference effects through superconducting point contacts", *Phys. Rev*. **141**, 367 (1966).

[5] J. Clarke, "A superconducting galvanometer employing Josephson junction", *Phil. Mag*. **13**, 115 (1966).

[6] J. Clarke, „Measurement of small voltages using a quantum interference device", in *Proc. on the Physics of Superconducting Devices*, B.S. Deaver, Jr., and W.S. Goree (Eds), Univ. of Virginia, Charlottesville (1967).

[7] J. Clarke, Doctoral Dissertation (1968), private communication (unpublished).

[8] K. K. Likharev, B. T. Ulrich, *Systems with Josephson Junctions* (in Russian), Moscow University (1978).

[9] K.K. Likharev, *Dynamics of Josephson Junctions and Circuits*, Gordon and Breach Science Publ., New York (1986).

[10] V.K. Kornev, K.K. Likharev, O.V. Snigirev, YE.S. Soldatov, V.V. Khanin, "Microwave-frequency SQUID with a high-Q dielectric resonator" (in Russian), *Radiotechn. & Electronics*, No. 12, 2647 (1980); English translation available in *1349 Radio Eng. & Electr. Physics*, p. 122 (1982).

[11] Elekta Neuromag, Siltasaarenkatu18 - 20 A, Helsinki, Finland; Mailing address: P.O. Box 68, FIN-00511 Helsinki, Finland; http://www.elekta.com/healthcare_international_elekta_neuromag.php.

[12] H. Seppä, "DC SQUID electronics based on adaptive noise cancellation and a high open-loop gain controller". In *Superconducting Devices and their Applications,* H. Koch and H. Lübbig (Eds.), Springer-Verlag, Berlin 2002, p. 346.

[13] H. Seppä, A. Ahonen, J. Knuutila *et al.*, „Dc SQUID electronics based on adaptive positive feedback: experiments", *IEEE Trans. Magn*. **27**, 2488 (1991).

[14] D. Drung, R. Cantor, M. Peters, T. Ryhänen, H. Koch, "Integrated magnetometer with high dV/dB", *IEEE Trans. Magn*. **27**, 3001 (1991).

[15] D. Drung, R. Cantor, M. Peters, H.J. Scheer, H. Koch, „Low-noise, high-speed dc superconducting quantum interference device magnetometer with simplified feedback electronics", *Appl. Phys. Lett*. **57**, 406 (1990).

[16] M. Mück, C. Heiden, "Planar microwave biased rf SQUIDs in niobium technology", *Appl. Phys*. (A) **54**, 475 (1992).

[17] C. Granata, A. Vettoliere, M. Russo, "Integrated dc-SQUID magnetometer in multichannel systems for biomagnetic imaging", *Proc. EUROCON 2007* (IEEE Catalog No. 07EX1617C, ISBN 1-4244-0813-X), pp. 556-563.

[18] S.M.Frolov, M.J.A.Stoutimore, T.A.Crane, D.J.Van Harlingen, V.A.Oboznov, V.Ryazanov,A.Ruosi, C.Granata, and M.Russo, "Imaging spontaneous currents in superconducting arrays of π-junctions*", Nature Physics* **4**, 32-36 (2008).

[19] R.J.P. Bain, G.B. Donaldson, S. Evanson, G. Hayward, "SQUID gradiometric detection of defects in ferromagnetic structures", in H.D. Hahlbohm and H. Lübbid (Eds), *SQUID'85, Proc. 3rd Intl. Conf. on Superconducing Quantum Devices*, deGruyter, Berlin (1985), p. 841.

[20] H.E. Hoenig, "SQUID arrays for biomagnetic diagnosis", *Physica Scripta* **T35**, 177 (1991); http://www.iop.org/EJ/article/1402-4896/1991/T35/038/physscr1_T35_038.pdf?request-id=aef6ada3-0504-408d-b213-29727da2dfb8.

[21] SUPRACON, AG, Wildenbruchstr.15, D-07745 Jena, Germany; info@supracon.com.

[22] C. M. Pegrum, G. B. Donaldson, A. H. Carr and A. Hendry, "Observation of quantum interference effects and SQUID operation in a bulk sample of YBaCuO at 77K and 4.2K", *Appl. Phys. Lett*. **51**, 1364 (1987).

[23] Y. Zhang, J. Schubert and N. Wolters, „Substrate resonator for HTS rf SQUID operation", *Physica* **C 372-376**, 282 (2002).

[24] M.I. Faley, U. Poppe, K. Urban, D.N. Paulson, T.N. Starr, R.L. Fagaly, "Low noise HTS dc SQUID flip-chip magnetometers and gradiometers", *IEEE Trans. Appl. Supercond*. 11, 1383 (2001), and references therein.

[25] Tristan Technologies, Inc., 6185 Cornerstone Court East, Suite 106, San Diego, CA 92121 USA; http://www.tristantech.com/.

[26] J. Kurkijärvi, "Intrinsic fluctuations in a superconducting ring closed with a Josephson junction", *Phys. Rev.* B **6**, 832 (1972).

[27] V.V. Danilov, K.K. Likharev, O.V. Snigirev, "Signal and noise parameters of SQUIDs". In *SQUID'85, Proc. 3rd Intl. Conf. on Superconducing Quantum Devices*, H.D. Hahlbohm and H. Lübbid (Eds), deGruyter, Berlin (1985), p. 473.

[28] C. Hilbert and J. Clarke, "SQUIDs as radio frequency amplifiers", *J. Low Temp. Phys*. **61**, 263 (1985).

[29] M. Mück, M.-O André, J. Clarke, J. Gail, Ch. Heiden, "Radio frequency amplifier based on a niobium dc SQUID with microstrip input coupling", *Appl. Phys. Lett*. **72**, 2885 (1998).

[30] M. Mück, C. Welzel and J. Clarke, " SQUID amplifiers at gigahertz frequencies", *Appl. Phys. Lett*. **82**, 3266 (2003), and references therein.

[31] M. Mück, J.B. Kycia, J. Clarke, "SQUID as a near-quantum-limited amplifier at 0.5 GHz", *Appl. Phys. Lett*. **78**, 967 (2001).

[32] P. Guttmann, "Dc SQUID with high energy resolution", *Electronics Lett*. **15**, 372 (1979).

[33] F.L. Vernon, R.J. Pederson, "Relaxation oscillations in Josephson junctions" *J. Appl. Phys*. **39**, 2661 (1968).

[34] C.D. Tesche, J. Clarke, "Dc-SQUID: noise and optimization", *J. Low Temp. Phys*. **27**, 301 (1977).

[35] M.W. Cromar, P. Carelli, "Low-noise tunnel junction dc SQUID's", *Appl. Phys. Lett*. **38**, 723 (1981).

[36] B. Chesca, „Analytical theory of DC SQUIDs operating in the presence of thermal fluctuations". *J. Low Temp. Phys*. 112, 165 (1998).

[37] B. Chesca, „Theory of RF SQUIDs operating in the presence of large thermal fluctuations", *J. Low Temp. Phys*. **110**, 963 (1998).

[38] X.H. Zeng, Y. Zhang, B. Chesca *et al.*, « Experimental study of amplitude-frequency characteristics of high-T_c rf SQUID", *J. Appl. Phys*. **88** 6781 (2000).

[39] B. Chesca, R. Kleiner, D. Koelle, "SQUID theory" in *The SQUID Handbook*, J. Clarke and A.I. Braginski (Eds.), Wiley-VCH, vol. I,II, (2004 nad 2006), pp. 50-59.

[40] D. Koelle, R. Kleiner, F. Ludwig, E. Dantsker, J. Clarke, „High-transition-temperature SQUIDs", *Rev. Mod. Phys*. **71**, 631 (1999),

[41] R. Kleiner, D. Koelle, J. Clarke, "A numerical treatment of the rf SQUID: I. General properties and energy resolution", *J. Low Temp. Phys*., **149**, 230-260, (2007).

[42] R. Kleiner, D. Koelle and John Clarke, "A numerical treatment of the rf SQUID: II. Noise temperature", *J. Low Temp. Phys*. **149**, 261-293, (2007).

[43] G. Testa, E. Sarnelli, S. Pagano, C.R. Calidonna, M.M. Furnari, „Characteristics of asymmetric superconducting quantum interference devices", *J. Appl. Phys*. **89**, 5145 (2001).

[44] P. Carelli, M.G. Castellano, K. Flacco et al., "An absolute magnetometer based on dc superconducting quantum interference devices", *Europhys. Lett*. **39**, 569 (1997).

[45] L.L. Sohn, M.T. Tuominen, M.S. Rzchowski *et al*., "Ac and dc properties of Josephson junctions arrays with long-range interaction", *Phys. Rev*. **B 47**, 975 (1993).

[46] J. Oppenländer, Ch. Häussler and N. Schopohl, Non-Φ_0-periodic macroscopic quantum interference in one-dimensional parallel junction arrays with unconventional grating structure, *Phys. Rev*. **B 63**, 024511 (2000).

[47] J. Oppenländer, Ch. Häussler and N. Schopohl, „Nonperiodic flux-to-voltage conversion of series arrays of dc superconducting quantum interference devices, *J. Appl. Phys*. **89**, 1875 (2001).

[48] J. Oppenländer, T. Träuble, C. Häussler, N. Schopohl, "Superconducting multiple loop quantum interferometers", *IEEE Trans. Appl. Supercond*. **11**, 1271 (2001).

[49] J. Oppenländer, C. Häussler, T. Träuble, N. Schopohl, „Highly sensitive magnetometers for absolute magnetic field measurements based on quantum interference filters", *Physica* **C 368**, 119 (2002).

[50] D. Doenitz, R. Straub, R. Kleiner, D. Koelle, „Microscopic analysis of low-frequency flux noise in YBCO dc SQUIDs", *Appl. Phys. Lett*. **85**, 5938 (2004).

[51] R. Humphreys, "Vortices in HTS junctions and SQUIDs", *IEEE Trans. Appl. Supercond*. **9**, 3741 (1999).

[52] M. Khapaev, M. Kupriyanov, E. Goldobin, M. Siegel, "Current distribution simulation for superconducting multi-layered structures", *Supercond. Sci. Technol*. **16**, 24 (2003).

[53] J.M. Rowell, M. Gurvitch, J. Geerk, "Modification of tunneling barriers on Nb by a few monolayers of Al", *Phys. Rev*. **B 24**, 2278 (1981); also following publications by Gurvitch *et al*. , 1981-1983.

[54] J.M. Jaycox, M.B. Ketchen, " Planar coupling scheme for ultra low noise dc SQUIDs", *IEEE Trans. Magn*. **MAG-17**, 400 (1981).

[55] J.E. Zimmerman, "Sensitivity enhancement of SQUIDs though the use of fractional-turn loops", *J. Appl. Phys*. **42**, 4483 (1971).

[56] P. Carelli, V. Foglietti, R. Leoni, M. Pullano, "Reliable low-noise dc SQUID", *IEEE Trans. Magn*. **25**, 1026 (1989).

[57] D. Drung, H. Koch, "An integrated dc SQUID magnetometer with variable positive feedback", *Supercond. Sci. Technol*. **7**, 242 (1994).

[58] B. David, D. Grundler, S. Krey, S., *et al*., „High-T_c SQUID magnetometers for biomagnetic measurements", *Supercond. Sci. Technol*. **9**, 96A-99A (1996).

[59] H. Seppä, M. Kiviranta, L. Grönberg, "dc SQUID based on unshunted junctions: experimental results", *IEEE Trans. Appl. Supercond*. **5**, 3248 (1995).

[60] D. Dimos, P. Chaudhari, J. Mannhart, "Superconducting transport properties of grain boundaries in YBCO bicrystals", *Phys. Rev*. **B 41**, 4038 (1990).

[61] J. Gao, Y. Boguslavskii, B.B. Klopman *et al*., "YBCO/PrBCO/YBCO Josephson ramp junctions, *J. Appl. Phys*. **72**, 575 (1992), and references therein.

[62] T. Ryhänen, H. Seppä, R. Cantor, „Effect of parasitic capacitance and conductance on the dynamics and noise of dc SQUIDs", *J. Appl. Phys*. **71**, 6150 (1992).

[63] J. Knuutila, A. Ahonen, C. Tesche, „Effects on dc SQUID characteristics of damping of input coil resonances", *J. Low Temp. Phys*. **68**, 269 (1987).

[64] J. Knuutila, M. Kajola, H. Seppä, R. Mutikainen, J. Salmi, "Design, optimization and construction of a dc SQUID with complete flux transformer circuits", *J. Low Temp. Phys*. **71**, 369 (1988).

[65] T. Ryhänen, H. Seppä,R. Ilmonieni, J. Knuutila, „SQUID magnetometers for low-frequency applications", *J. Low Temp. Phys*. **76**, 287 (1989).

[66] H. Seppä, M. Kiviranta, A. Satrapinski, "A coupled dc SQUID with low 1/f noise", *IEEE Trans. Appl. Supercond*. **3**, 1816 (1993).

[67] H. Seppä, T. Ryhänen, "Influence of the signal coil on the SQUID dynamics", *IEEE Trans. Magn.* **MAG-23**, 1083 (1987).

[68] E.J. Tarte, D.J. Kang, W.E. Booij *et al*., „Improvement of high-T_c SQUID performance using an integrated resistor", *IEEE Trans. Appl. Supercond*. **9**, 4432 (1999).

[69] J. Penttilä, L. Grönberg, J. Hassel, M. Kiviranta, „Optimized SQUID sensors for low-frequency measurements", Proc. LT 25, to appear online in *J. Phys. Conf. Series* (2009).

[70] G.B. Donaldson, M.B. Ketchen, J. Clarke, W. Goubau, "An integrated thin-film gradiometer based on a dc SQUID", in *SQUID '76,* H.D. Hahlbohm and H. Lübbig, (Eds.), Walter de Gruyter, Berlin (1976), p. 4111.

[71] A.I. Ahonen, M.S. Hämäläinen, M.J. Kajola *et al.*, "122-channel SQUID instrument for investigating magnetic signals from the human brain", *Physica Scripta* **T49**, 198 (1993).

[72] R. Stolz, L. Fritzsch, H.-G. Meyer, „LTS SQUID sensor with a new configuration", *Supercond. Sci Technol.* **12**, 806 (1999).

[73] V. Schultze, R. Ijseelseijn, T. May, H.-G. Meyer, "Highly balanced single-layer high-temperature superconductor SQUID gradiometer freely movable within the Earth's magnetic field", *Supercond. Sci. Technol.* **16**, 773 (2003).

[74] S. Knappe, D. Drung, T. Schurig *et al.*, A planar YBCO thin-film gradiometer operating at 77 K", *Cryogenic*s **32**, 881 (1992).

[75] V. Zakosarenko, F. Schmidl, H. Schneidewind *et al.*, „Thin-film dc SQUID gradiometer using a single YBCO layer", *Appl. Phys. Lett.* **65**, 779 (1994).

[76] S. Wunderlich, F.Schmidl, H.Specht, *et al.*, „Planar gradiometers with high-T_c SQUIDs for non-destructive testing", *Supercond. Sci. Technol.* **11**, 315-321(1998).

[77] A. Eulenburg, E.J. Romans, C. Carr et al., Highly balanced long-baseline single-layer high-T_c SQUID gradiometer", *Appl. Phys. Lett.* **75**, 2301 (1999).

[78] C. Carr, E.J. Romans, A.J. Millar *et al.*, "First-order high-T_c single-layer gradiometers: parasitic effective area compensation and system balance", *IEEE Trans. Appl. Supercond.* **11**, 1367 (2001).

[79] V. Schultze, R. Ijselstein, H.-G. Meyer *et al.*, „High-T_c superconducting quantum interference filters for sensitive magnetometers",*IEEE Trans. Appl. Supercond.* 13, 775 (2003).

[80] V. Schultze, R. Ijselstein, H.-G. Meyer *et al.*, „Improved high-T_c superconducting quantum interference filters for sensitive magnetometers", *Supercond. Sci. Technol.* **16**, 1356 (2003).

[81] V. K. Kornev, I. I. Soloviev, J. Oppenlaender, *et al.*, "Oscillation linewidth and noise characteristics of parallel SQIF," *Superconductor Science and Technology*, **17**, S406 (2004).

[82] V. K. Kornev, I. I. Soloviev, N. V. Klenov, O. A. Mukhanov, "High-linearity SQIF-like Josephson Junction Structures", submitted to *IEEE Trans. Appl. Supercond.* 19 (2009).

[83] N. Schopohl, private communication (unpublished).

[84] P. Caputo, J. Oppenländer, Ch. Häussler *et al.*, „High-performance magnetic field sensor based on superconducting quantum interference filters", *Appl. Phys. Lett.* **85**, 1389 (2004).

[85] QEST, Quantenelektronische Systeme GmbH, Max-Eyth-Str. 38, 71088 Holzgerlingen, Germany; http://www.qest.de/index.html.

[86] V. Schultze, R. Ijselsteijn, H.-G. Meyer, „How to puzzle out a good high-T_c superconducting quantum interference filer", *Supercond. Sci. Technol.* **19**, S411 (2006).

[87] D. Drung, M. Mück, "SQUID Electronics" in *The SQUID Handbook,* J. Clarke and A.I. Braginski (Eds.), Wiley-VCH, Weinheim, vol. I,(2004) pp. 127-170.

[88] D. Drung, „High-T_c and low-T_c dc SQUID electronics", *Supercond. Sci. Technol.* **16**, 1320 (2003).

[89] Magnicon GbR, Lemsahler Landstr. 171, 22397 Hamburg, Germany; http://www.magnicon.com/squid- electronics/.

[90] D. Drung, C. Hinnrichs, H.-J. Barthelemess, „Low-noise ultra-high-speed dc SQUID readout electronics", *Supercond. Sci. Technol.* **19**, S235 (2006).

[91] M. Kiviranta, H. Seppä, "Dc SQUID electronics based on the noise cancellation scheme, *IEEE Trans. Appl. Supercond.* **5**, 2146 (1995).

[92] M. Kiviranta, "SQUID linearization by current-sampling feedback", *Supercond. Sci. Technol.* **21**, 045009 (2008).

[93] M. Mück, G. Hallmans, Ch. Heiden, M. Cerdonio, G. Fontana, R. Mezzena, S. Vitale, „Planar microvawe-biased rf SQUID using a cryogenic HEMT amplifier", *Appl. Phys. Lett.* **61**, 1231 (1992).

[94] M. Kiviranta, A. Virtanen, H. Seppä *et al.*, "A post-SQUID ac amplifier aimed for multiplexed detector circuits", *Supercond. Sci. Technol.* **19**, S371 (2006).

[95] M. Kiviranta, "Use of SiGe bipolar transistors for cryogenic readout of SQUIDs", *Supercond. Sci. Technol.* **19**, 1297 (2006).

[96] D. Drung, C. Assmann, J. Beyer, *et al.*, „Highly sensitive and easy-to-use SQUID sensors, *IEEE Trans. Appl. Supercond.* **17**, 699 (2007).

[97] D. Drung, J. Beyer, M. Peters, J. Storm, T. Schurig, „Novel SQUID current sensors with high linearity at high frequencies", *IEEE Trans. Appl. Supercond.* 19, No. 3 in press (2009).

[98] D. Drung, private communication (March 2009).

[99] M. Mück, Ch. Heiden, "Simple dc SQUID system based on a frequency-modulated relaxation oscillator", *IEEE Trans. Magn.* **25**, 1151 (1989).

[100] S.A. Gudoshnikov, O.V. Kaplunenko, Yu.V. Maslennikov, O.V. Snigirev, "Relaxation-oscillation-driven dc
    SQUIDs", *IEEE Trans. Magn*. **25**, 1178 (1989).
[101] D.J. Adlerhof, H. Nijstad, J. Flokstra, H. Rogalla, "(Double) relaxation oscillation SQUIDs with high flux-to-voltage transfer: simulations and experiments", *J. Appl. Phys*. **76**, 3875 (1994).
[102] D.J. Adlerhof, J. Kawai, G. Uehara, H. Kado, "High sensitivity double relaxation SQUIDs with large transfer from flux to voltage", *Rev. Sci. Instrum*. **66**, 2631 (1995).
[103] T. Reich, P. Febvre, Th. Ortlepp *et al*., „Experimental study of a hybrid single flux quantum digital SQUID magnetometer", *J. Appl. Phys*. **104**, 024509 (2008).
[104] The Fluxonics Foundry; http://www.fluxonics-foundry.de.